Supporting Information: Flash Lamp Annealing Enables Dislocation Density Reduction and Probing of Defect Dynamics in Epitaxial Germanium for On-Chip Integration

Andrea Giunto,* Joel Reñé Sapera, Shelly Ben David, Thomas Hagger, Santhanu Panikar Ramanandan, and Anna Fontcuberta i Morral†
Laboratory of Semiconductor Materials, Institute of Materials, École Polytechnique Fédérale de Lausanne, Lausanne, Switzerland

Victor Boureau
Interdisciplinary Center for Electron Microscopy (CIME), École Polytechnique Fédérale de Lausanne, Lausanne, Switzerland

Arianna Nigro, Cedric Gonzales, and Ilaria Zardo
Physics Department, University of Basel, Klingelbergstrasse 82, CH-4055 Basel, Switzeland

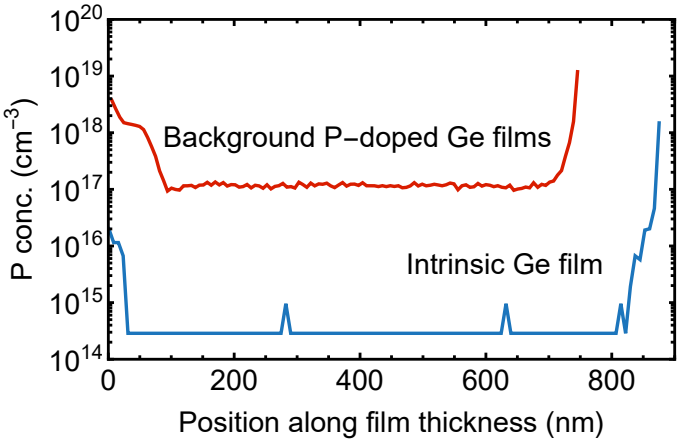

FIG. S1. **Secondary-ion mass spectroscopy (SIMS) characterization of background doping in Ge:P films.** Phosphorus (P) concentration profiles for (red) *Ge:P740* and (blue) an intrinsic Ge sample—grown in the same conditions as *Ge440*—films. The background P concentration in *Ge:P740* is $1.14 \times 10^{17}\,\mathrm{cm}^{-3}$, whereas in *Ge440* it lies below the detection limit of $3 \times 10^{14}\,\mathrm{cm}^{-3}$. All Ge:P films in this study were grown sequentially, following several intrinsic Ge growths, with no other growths or operations performed in the chamber in between. Analogous background P concentrations are therefore expected in *Ge:P421* and *Ge:P2475*.

* andrea.giunto@epfl.ch
† anna.fontcuberta-morral@epfl.ch

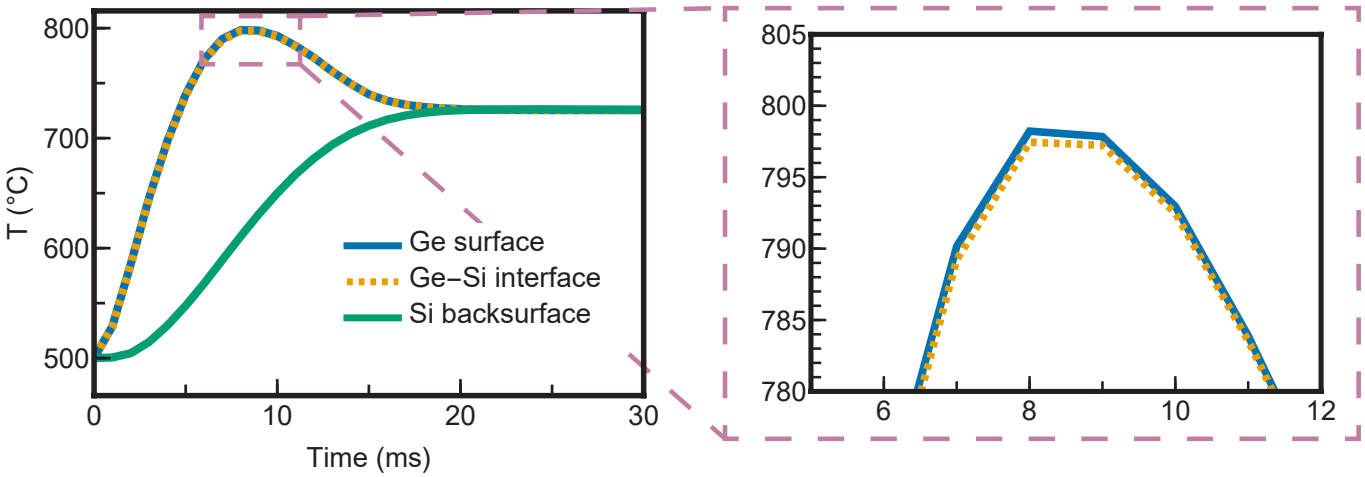

FIG. S2. **COMSOL simulation of the temperature profile during FLA in a 740 nm Ge film.** The data of Fig. 1(b) are complemented with the profile at the Si–Ge interface, showing a peak-temperature difference of only ∼1°C between surface and interface (see zoomed view).

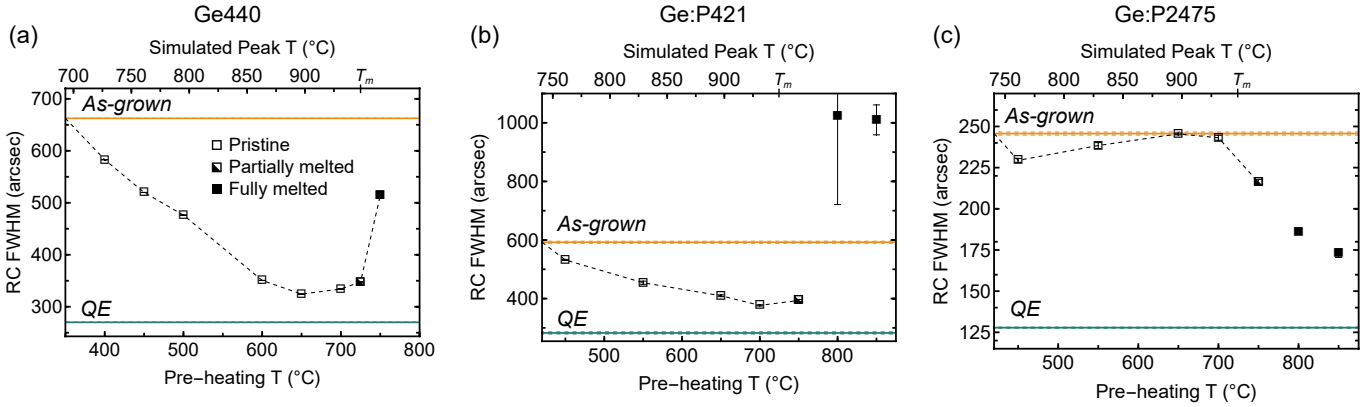

FIG. S3. **Single-pulse flash-lamp annealing of epitaxial Ge.** Rocking curve (RC) full width at half maximum (FWHM) of the XRD Ge(004) peak after a single FLA pulse (7.65 ms, 48.1 J/cm^2) as a function of pre-heating temperature, varied from 400 °C to 850 °C. Panels correspond to different samples from Tab. I: **(a)** *Ge440*; **(b)** *Ge:P421*—both showing trends analogous to *Ge:P740* in Fig. 2(a); and **(c)** *Ge:P2475*, which exhibits a slightly different trend. The origin of this deviation was not further investigated, as the multiple-pulse results of *Ge:P2475* (Fig. 5(a)) are analogous to those of the other samples.

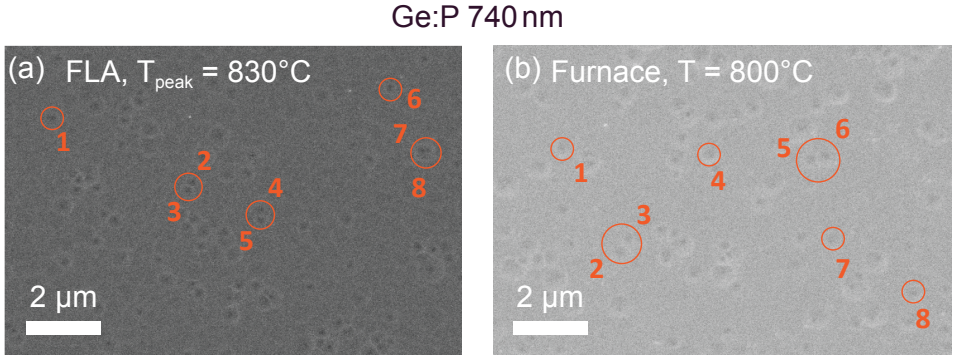

FIG. S4. **Representative SEM images of etched surfaces of annealed *Ge:P740* films during etch-pit density (EPD) characterization of TDD.** (**a**) Film annealed with 500 FLA pulses at T_{peak} = 830 °C. (**b**) Film annealed using conventional long-duration annealing (800 °C, 45 min) to reach its quasi-equilibrium state. A few selected etch pits are marked as examples to illustrate the pit-counting procedure. EPD yields equivalent TDD for the two films, respectively (**a**) (6.55 ± 0.66) × 10^7 cm^{-2} and (**b**) (6.30 ± 0.52) × 10^7 cm^{-2}.

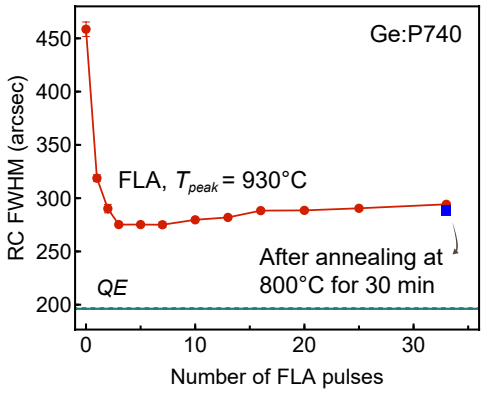

FIG. S5. **Irreversibility of stacking fault (SF) formation.** Evolution of the RC FWHM in *Ge:P740* after multiple FLA pulses at T_{peak} = 930°C (red curve, extracted from Fig. 3(a)). The plateau RC FWHM value is significantly higher than the QE FWHM, consistent with the formation of SFs observed in Fig. 4. The blue square marks the RC FWHM measured on the same sample—after exposure to 33 FLA pulses—following conventional annealing at 800°C for 30 min. While the latter annealing conditions allow to reach the QE defect level in *as-grown* samples, they do not significantly reduce the RC FWHM in this sample after high-temperature FLA exposure, indicating that SF formation is irreversible.

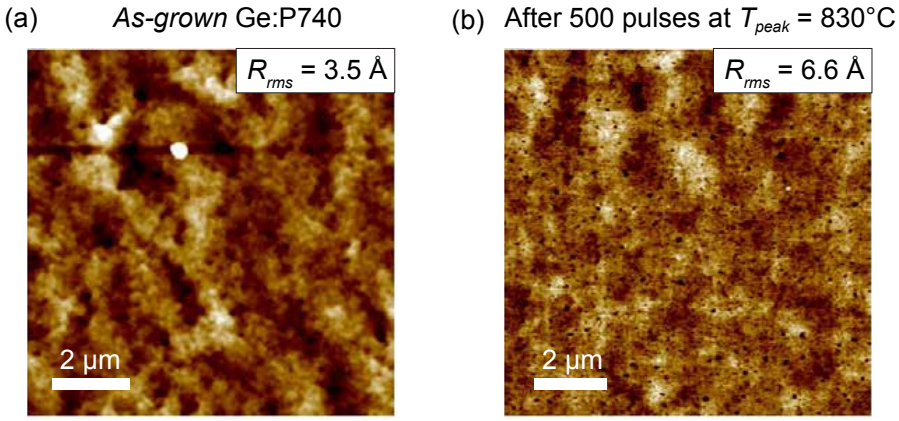

FIG. S6. **AFM characterization of surface roughness of Ge films.** Root mean square roughness (R_{rms}) measurements of (**a**) *as-grown Ge:P740*, and (**b**) the same film after 500 FLA pulses at T_{peak} = 830°C, showing values of respectively 3.5 Å and 6.6 Å. The R_{rms} in (**a**) was computed selecting a region without the white surface defect.

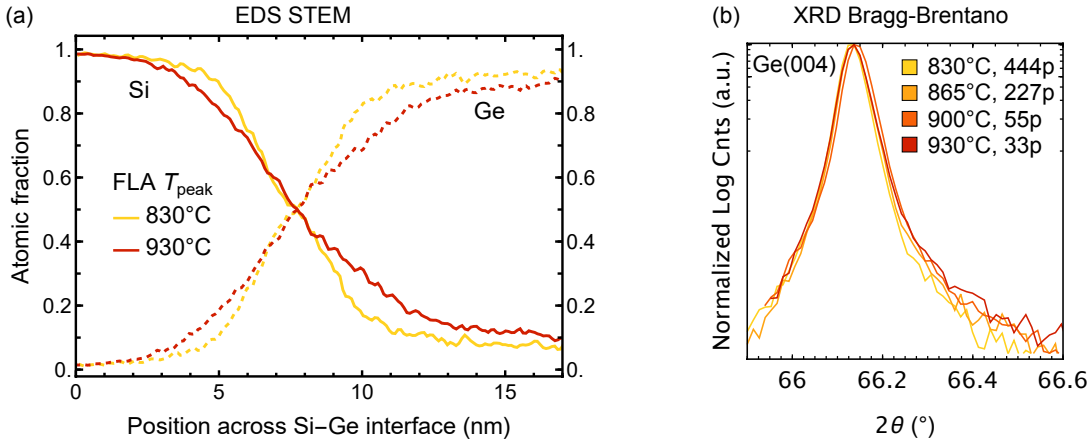

FIG. S7. **Comparison of Si–Ge intermixing induced by different numbers of FLA pulses and pre-heating temperatures.** (**a**) Si/Ge atomic fraction profiles across the Si–Ge interface in the *Ge:P740* film annealed under different conditions (as in Fig. 4), as measured by energy-dispersive x-ray spectroscopy (EDS) in STEM. The yellow curve corresponds to a film annealed with 500 pulses at $T_{peak} = 830$°C, and the red curve to 33 pulses at $T_{peak} = 930$°C. Si and Ge atomic fractions are plotted respectively as continuous and dashed lines. The extent of intermixing in the two films is comparable, with slight deviations in the Si/Ge ratio confined to 10 nm around the interface over a total film thickness of 740 nm. (**b**) Ge(004) XRD peaks measured in symmetrical Bragg–Brentano geometry for *Ge:P740* films FLA-annealed under the conditions listed in the legend, where *p* stands for *pulses*. The high-angle shoulder indicates partial Si intermixing, consistent with EDS STEM measurements, and is similar across all four films (note the *log* scale on the y axis) as a result of the higher number of pulses applied at lower pre-heating temperatures.

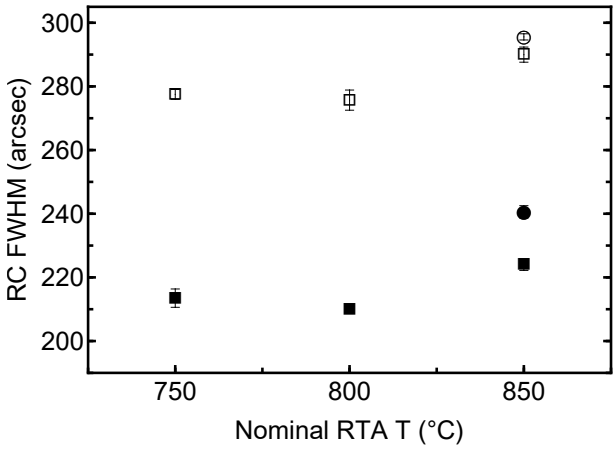

FIG. S8. **Rapid thermal annealing (RTA) of epitaxial Ge showing increased defect density at excessive annealing temperatures.** XRD RC FWHM of Ge(004) after RTA at 750, 800, and 850°C. Empty and solid symbols correspond to Ge:P films grown under the same conditions as *Ge:P421* and *Ge:P740*; small thickness variations may arise from Ge cell effusivity in MBE. Annealing was performed with a 20°C/s heating ramp and 5 min dwell in $N_2 + 5\%H_2$, without capping. The temperature was monitored with a thermocouple in contact with the backside of the Si support wafer, on which the chips were placed. Samples were cooled either by switching off the lamps (squares) or at 40°C/min to 600°C before uncontrolled cooling (circles). Each data point represents two chips; error bars were computed as described in the main text. For both thicknesses, the FWHM decreases from 750°C to 800°C, indicating that 750°C/5 min is insufficient to reach the films' QE FWHM. At 850°C, the FWHM increases, consistent with MDs splitting into SFs and partial dislocations at excessive annealing temperatures. To test whether this increase could stem from the high cooling rates in FLA or uncontrolled RTA, we repeated the annealing at 850°C with slower cooling (circles). This did not reduce FWHM; instead, it yielded a slightly larger value, whose origin remains unclear.

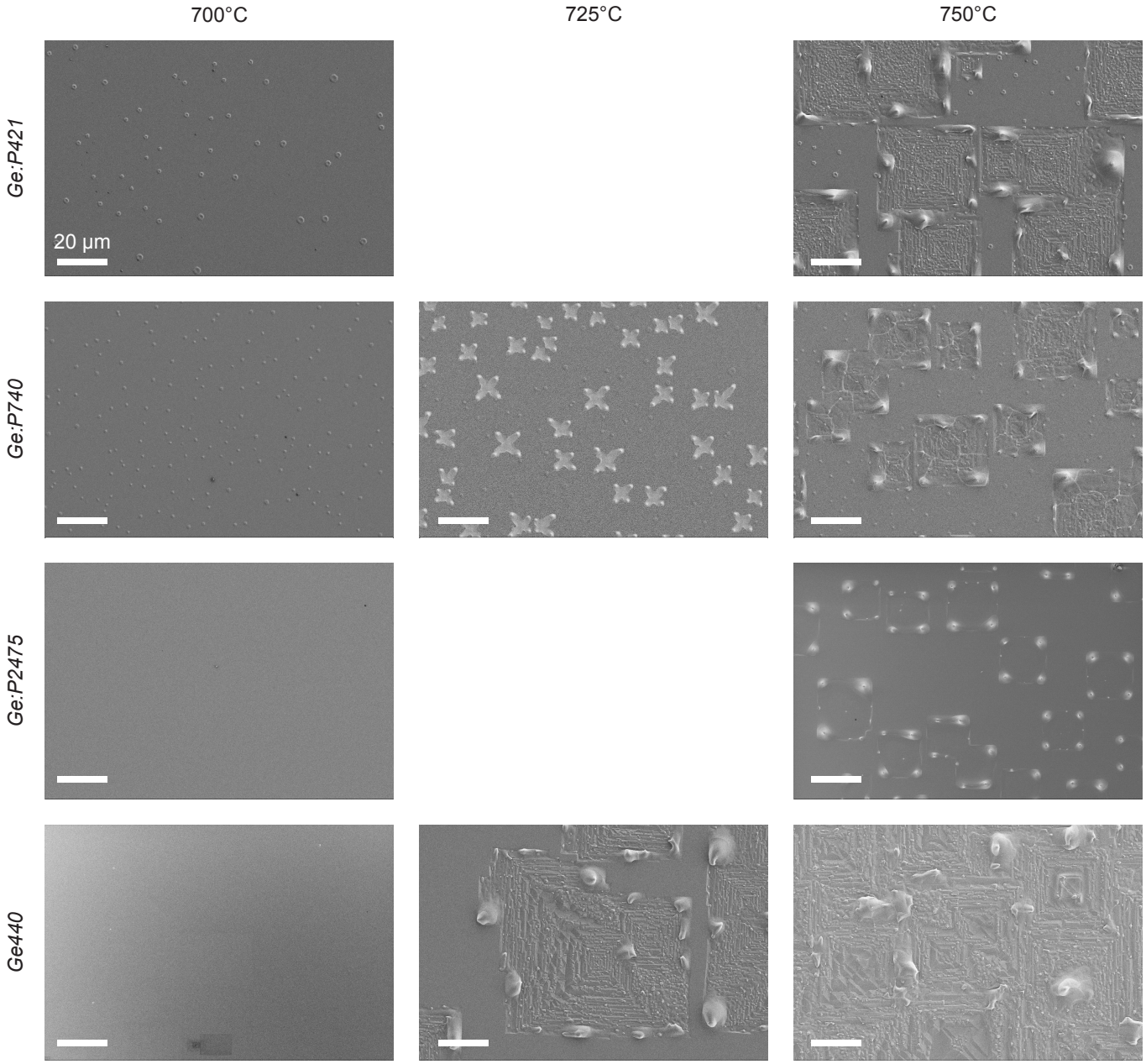

FIG. S9. **Onset of Ge melting during FLA as a function of pre-heating temperature.** Top-view secondary-electron SEM images of Ge films (Tab. I) after a single FLA pulse of 7.65 ms, 48.1 J/cm^2 with nominal pre-heating at 700, 725, and 750°C. No melting is observed at 700°C, while it is evident at 750°C. At 725°C, tested on two samples, partial melting occurs and this temperature was therefore used as reference to calibrate COMSOL Multiphysics® temperature simulations. Surface features visible at 700°C in *Ge:P421* and *Ge:P740* are not a result of annealing; they originate from substrate defects and are also present in as-grown films.